



**HAL**  
open science

## Monte Carlo simulation of collimated beam transmission through turbid media

S. Avrillier, E. Tinet, E. Delettre

### ► To cite this version:

S. Avrillier, E. Tinet, E. Delettre. Monte Carlo simulation of collimated beam transmission through turbid media. *Journal de Physique*, 1990, 51 (22), pp.2521-2542. 10.1051/jphys:0199000510220252100 . jpa-00212551

**HAL Id: jpa-00212551**

**<https://hal.science/jpa-00212551>**

Submitted on 4 Feb 2008

**HAL** is a multi-disciplinary open access archive for the deposit and dissemination of scientific research documents, whether they are published or not. The documents may come from teaching and research institutions in France or abroad, or from public or private research centers.

L'archive ouverte pluridisciplinaire **HAL**, est destinée au dépôt et à la diffusion de documents scientifiques de niveau recherche, publiés ou non, émanant des établissements d'enseignement et de recherche français ou étrangers, des laboratoires publics ou privés.

Classification  
Physics Abstracts  
42.10 — 42.20

## Monte Carlo simulation of collimated beam transmission through turbid media

S. Avrillier, E. Tinet and E. Delettre

Laboratoire de Physique des Lasers, Université Paris XIII, 93430 Villetaneuse, France

(Received 26 February 1990, revised 16 July 1990, accepted 20 July 1990)

**Résumé.** — La transmission ( $T$ ) et la réflexion ( $R$ ) d'un milieu homogène diffusant la lumière de façon isotrope sont calculées numériquement à l'aide d'une simulation dite de Monte Carlo (MC), dans le cas d'un faisceau incident parallèle. Un grand nombre de valeurs des coefficients d'absorption  $\kappa$  et de diffusion  $\sigma$  par unité de longueur ont été explorées de façon à couvrir pratiquement tous les cas possibles. Nous présentons ces résultats MC sous forme de réseaux de courbes avec des paramètres réduits, ce qui permet d'avoir une vision globale des phénomènes. Ces résultats précis nous ont permis de délimiter les domaines de validité des expressions analytiques approchées obtenues avec un modèle à trois flux ou par résolution de l'équation de transfert radiatif. Enfin nous avons construit des abaques simples à utiliser pour la détermination graphique directe des coefficients  $\kappa$  et  $\sigma$  à partir des mesures de  $R$  et  $T$ . Les effets des réflexions sur les surfaces du milieu sont discutés dans la dernière partie de l'article.

**Abstract.** — An accurate Monte Carlo (MC) computer model is used to calculate the reflectances ( $R$ ) and transmittances ( $T$ ) of isotropic scattering media for the case of collimated beam illumination and for a wide range of absorption and scattering coefficients  $\kappa$  and  $\sigma$  per unit length. The MC results are presented by means of sets of curves with distance scaling in order to give an overall understanding of the subject. Numerical comparisons are made with analytical expressions obtained with a 3-flux model or derived from the equation of radiative transfer. These comparisons indicate the range of  $\kappa$  and  $\sigma$  values where these expressions are applicable. A simple diagram is constructed with accurate MC results and can be used for direct graphical determination of  $\kappa$  and  $\sigma$  from  $R$  and  $T$  measurements. The effects of reflections at the boundaries are described in the last section.

### 1. Introduction.

Light propagation in scattering and absorbing media has received considerable attention. The study of this phenomenon requires two strongly related steps :

- 1) an experimental determination of the optical properties of the medium of interest ;
- 2) the development of a suitable theory or model for describing the light propagation in the medium.

Up to now experimental methods used to determine the scattering and absorption characteristics of a medium are mostly based on measurements of the reflectance and transmittance of slabs of the material. The most typical technique make use of spec-

trophotometers with integrating spheres. For example, for measuring transmittance, the sample is placed on an aperture made in the integrating sphere and is irradiated either by a collimated beam or by diffuse light coming from a flux-filled second integrating sphere (Fig. 1). Obviously reflectance cannot be measured by this twin-spheres technique, and the sample is typically irradiated unidirectionally by a collimated beam through a small opening in the collecting sphere. Successive measurements can be made with an incident beam at various angles to the normal to the sample surface.

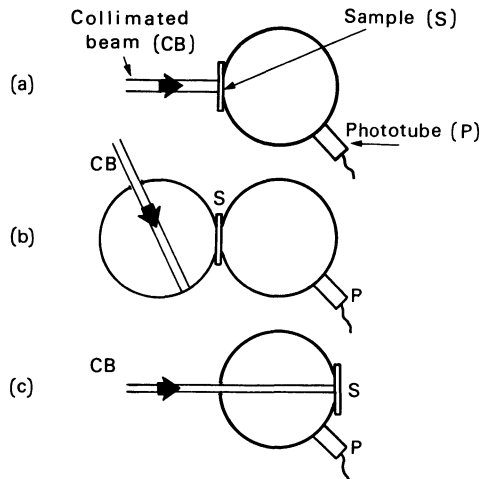


Fig. 1. — Some examples of integrating spheres apparatus for transmittance or reflectance measurements. (a) Measurement of the transmittance of a sample illuminated by a collimated beam. (b) Measurement of the transmittance of a sample illuminated by diffuse light coming from a flux-filled second integrating sphere. (c) Measurement of the reflectance of a sample illuminated by a collimated beam.

Alternative methods based on measurements of the spatial distribution of the reflected light have been recently proposed [1, 2].

As far as theory is concerned, several approaches have been developed. The aim of these has been to find analytical expressions which are more satisfactory for the physicists and can be computed very rapidly.

The most popular are the 2, 4 or  $n$ -flux phenomenological models initiated by Kubelka [3, 4] and the methods of solving the equation of radiative transfer [5-7].

Although these theories are often well founded, in practice many assumptions are used to simplify the mathematics. A variety of more or less approximate analytical solutions has been constructed within the conditions encountered in the measurements :

- the sample is bounded by parallel planes, the dimensions of which are very large compared to the sample thickness ;
- the medium is homogeneous or made of several optically different homogeneous layers ;
- in many cases the incident light is assumed to be collimated or perfectly diffuse.

A good analytical description is obtained for the limiting cases of dominant absorption or dominant scattering but it is much more complicated to deal with the intermediate cases where both absorption and scattering processes are significant.

Incorporating real conditions such as source geometry, anisotropic phase function, reflections on surfaces, inhomogeneous medium, is also very difficult and makes the mathematical treatment very complicated. Numerical treatments are very often necessary to solve the equations [6, 7].

Many papers compare the results of various theories and discuss their conditions of validity but it is still very difficult to get a comprehensive understanding of light propagation in a scattering medium even in the simplest cases.

An other and more general theoretical approach is to use a numerical Monte Carlo (MC) simulation to follow the photons along their pathways in the material [1, 8, 9]. The algorithm is very simple and MC calculations can be used for more realistic geometries without additional conceptual difficulties. The main disadvantage of this method lies in its large computer calculation time. The more real conditions are taken into account, the more time is required to obtain accurate results. Nevertheless commercially available personal computers have recently become quite powerful and now allow the use of this method in laboratories.

The object of this paper is both to test the accuracy of numerical MC simulations and to give an overall and precise knowledge of diffuse reflection and transmission of light by absorbing and scattering media in simple cases. Thus we present results of MC calculations for a plane-parallel slab illuminated by a parallel beam of monochromatic light in the case of isotropic scattering which is encountered, for example, when the scattering particles are spherical and very small compared with the wave length. Accurate values of the transmittance  $T$  and reflectance  $R$  are given for a very large range of absorption and scattering coefficients per unit length  $\kappa$  and  $\sigma$  and for various slab thicknesses  $d$  in order to cover nearly all possible cases. When possible, these values are compared with accurate values already available in the tabulations by Van De Hulst [6] and Giovanelli [22] in the matched boundary case.

These general results are presented by means of sets of curves using distance scaling and reduced parameters so that they may be used with any sample.

In the most simple cases we compare the accurate results of MC calculations to those obtained with some approximate analytical expressions derived from a 3-flux model or from solving the equation of radiative transfer and we determine their conditions of validity.

Graphical solutions for  $\kappa$  and  $\sigma$  in terms of experimentally observed  $T$  and  $R$  are presented parametrically in a simple graph. The general problem of this determination is widely discussed.

Effects of the reflections at the slab boundaries are discussed in section 4.

## 2. Monte Carlo method.

The Monte Carlo methods proceed in a very different way from the analytical methods. Light propagation in a scattering medium is not considered as a whole but is described locally : the photon defined by its space coordinates and its direction of propagation undergoes events which are mainly changes of direction in scattering events or its disappearance by absorption. The path length between two interactions is statistically dependent on the probability of each event.

The accuracy of the final result depends on the total number of photons used in the calculations. For computational efficiency it is in fact more convenient to use groups of photons rather than single photons.

All the photons of a same group are generated along the same incident ray and undergo the same changes of direction at the scattering points.

**2.1 MODELS.** — In a first type of Monte Carlo technique (MC1) [1] part of the photons of a group is absorbed continuously along the ray path between two scattering events and the

other photons continue to follow their natural histories. At each point of the pathway the weight of the group is equal to the number of unabsorbed photons which represents the probability for one photon to reach this point along this special trajectory.

In this way a large number of individual stories are explored at once.

The basic steps of our MC1 simulation are (Fig. 2) :

(1) a group of photons, of initial weight equal to 1, is generated with an incident direction perpendicular to the sample surface ;

(2) the path length between successive scattering events is calculated as

$$L = - \text{Ln} (r) / \sigma \tag{1}$$

where  $r$  is a random number uniformly distributed between 0 and 1 and  $\sigma$  is the true scattering coefficient per unit length, which is the product of the number density of scattering particles by the individual scattering cross section.  $\sigma$  is then the inverse of the elastic mean free path. This expression of  $L$  is statistically equivalent to the probability  $\exp[-\sigma L]$  for a photon to cover a distance  $L$  between two scattering events if no absorption occurs on this path ;

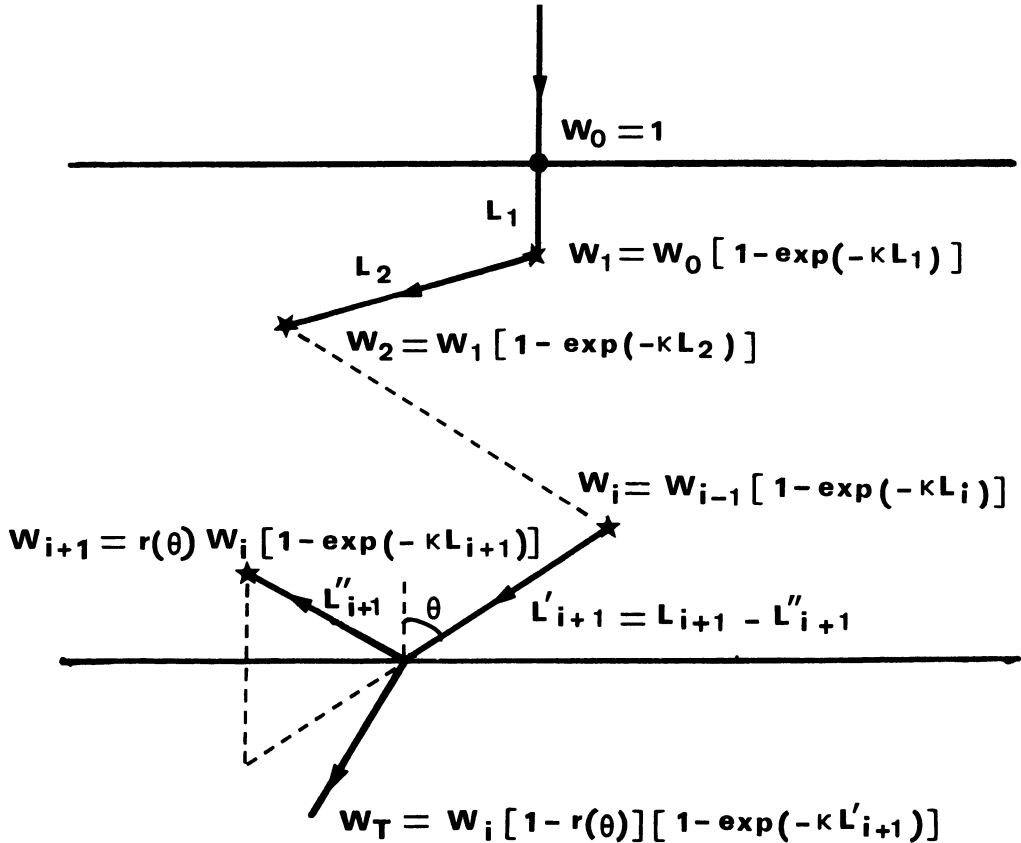


Fig. 2. — Schematic of a group of photons history showing the weighting factor at each interaction point for the MC1 Monte Carlo model.  $\kappa$  is the absorption coefficient and the  $L_i$  are the path lengths between successive scattering events. In case of specular reflection at the boundaries, the weight is multiplied by the reflection coefficient  $r(\theta)$  corresponding to the angle of incidence  $\theta$ . The refracted part of the light participates in  $R$  or  $T$  depending on the surface.

(3) along a path the absorption is taken into account by multiplying the weight of the group by  $\exp[-\kappa L]$  ;

(4) at the end of each path a new direction is determined. In order to reduce the number of significant parameters, we have investigated the case of isotropic scattering which has been widely studied in the literature. The extension of the MC methods to anisotropic scattering cases can be done without further complications by using, for example, a statistical law derived from the Henyey-Greenstein phase function [10, 1] ;

(5) non random events occur when the trajectory crosses one of the slab surfaces : part of the light is reflected towards the medium and in case of specular reflection it is easy to calculate its weight and its direction, the refracted part of the light participates in  $R$  or  $T$  depending on the surface ;

(6) groups of photons whose weight becomes lower than a critical weight, determined by the desired precision, are eliminated.

In a second type of Monte Carlo technique (MC2) [9] (Fig. 3) absorption is not treated as a continuous phenomenon but the group of photons is assumed to deposit a fraction of its

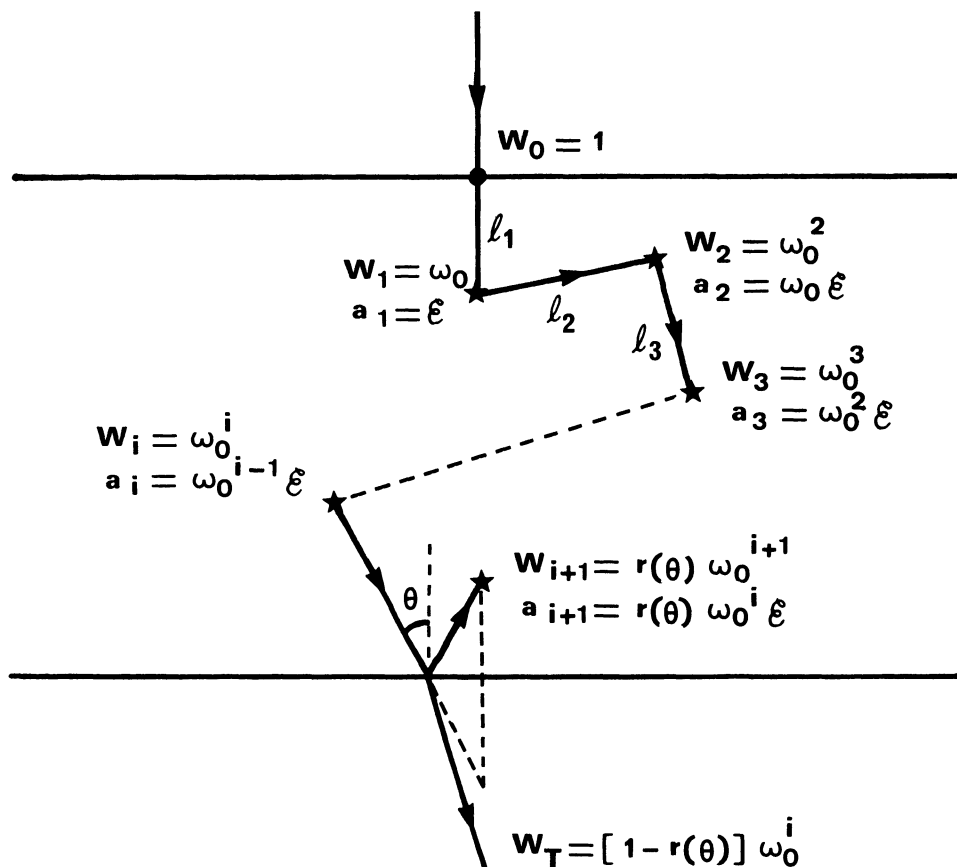


Fig. 3. — Schematic of a group of photons history showing the weighting factor  $W_i$  and the absorbed dose  $a_i$  at each interaction point for the MC2 Monte Carlo model.  $\omega_0$  is the sample scattering albedo and  $\epsilon = 1 - \omega_0$ . The  $l_i$  are the path lengths between successive scattering events. In the case of specular reflection at the boundaries, the weight is multiplied by the reflection coefficient  $r(\theta)$  corresponding to the angle of incidence  $\theta$ . The reflected part of the light participates in  $R$  or  $T$  depending on the surface.

weight, as absorbed energy, at each scattering point. Steps (2) and (3) of MC1 are modified for MC2 :

(2) the path length between successive interactions is calculated as :

$$\ell = -\text{Ln}(r)/(\kappa + \sigma) \quad (2)$$

(3) at each interaction point a fraction of the photons family equal to the simple scattering albedo  $\omega_0 = \sigma/(\kappa + \sigma)$  is scattered and a fraction  $\varepsilon = 1 - \omega_0 = \kappa/(\kappa + \sigma)$  is absorbed.

In our  $T$  and  $R$  calculations we have obtained exactly the same results with these two methods. This agreement is due to the fact that the absorption and diffusion phenomenons are described by the same probability laws in the two models. MC2 would be computationally more convenient for the calculation of the distribution of absorbed « dose » in the sample and is often less computer-time consuming.

**2.2 ACCURACY OF MC CALCULATIONS.** — Since the final result is obtained by averaging over the contributions of many photons, its accuracy depends on the number of photons used in the calculations.

In order to evaluate this accuracy, we have made, in many different cases, a statistical estimation of the variance of the results:  $R$  and  $T$  are calculated  $25 \times 10^3$  times with  $10^3$  groups of photons for a given set of  $\kappa$ ,  $\sigma$  and  $d$  values, where  $d$  is the thickness of the slab. The half width at  $1/e$  height of the quasi-Gaussian distribution of the results is always very close to  $1.6 \times 10^{-2}$  (absolute deviation) for  $T$  and very often much smaller than  $1.6 \times 10^{-2}$  for  $R$ .

To obtain a variance 10 times smaller, one should approximately multiply by 100 the number  $N$  of groups of photons used in the calculations.

From this study we can assume that the absolute deviation of the MC results from exact values is smaller than  $1.6 \times 10^{-2} \times (1000/N)^{1/2} = (0.26/N)^{1/2}$ . This assumption appeared to be verified each time we could compare our MC results to some very accurate values given in the litterature [6].

For the elimination of the photons, it is not necessary to use a cut off weight smaller than  $(0.26/N)^{1/2}$ .

The results presented in this paper have been computed with  $10^6$  groups of photons and a cut off weight equal to  $10^{-5}$ . The absolute statistical error is then  $\leq 5 \times 10^{-4}$  for  $T$ , and very often  $\ll 5 \times 10^{-4}$  for  $R$ , which, up to now, corresponds to the accuracy of the best experimental measurements.

### 3. Case of index matching of the medium to the environment.

The scattering medium of finite thickness  $d$  is supposed to be bounded by two infinite parallel planes. One of the planes is illuminated by a collimated normally incident beam.

In this paper, the results are limited to cases that satisfy the following conditions :

- (a) the medium is homogeneous, isotropic and linear ;
- (b) scattering is isotropic ;
- (c) the light intensity is low enough so that non linear effects can be neglected. The photons are assumed to be independent ;
- (d) the optical characteristics of the medium are not modified by the absorbed energy. The medium does not emit radiation or fluoresce ;
- (e) the radiation is monochromatic and the absorption and scattering coefficients  $\kappa$  and  $\sigma$  are constant in the medium.

One of the effects of this geometry and of these restrictions is that the total reflectance  $R$  and transmittance  $T$  do not depend on the intensity distribution in the incident collimated beam.

In the most simple case of index matching of the medium to the environment on the entrance and exit sides of the slab, no surface reflections occur.  $R$  and  $T$  depend only on the optical thickness  $(\kappa + \sigma) d$  and on the ratio  $\kappa/\sigma$  which can be used as a parameter. All results presented below have distances measured in units of the mean free path  $1/(\kappa + \sigma)$  in order to be shown in a more condensed and universal form.

3.1 MONTE CARLO RESULTS. — Some of the MC calculated values of transmittance  $T$  and reflectance  $R$  are given in table I and table II respectively.

The variations of  $T$  as a function of optical thickness are given in figure 4 for  $\kappa/\sigma$  ratios ranging from  $10^{-3}$  to  $2 \times 10^2$ .  $T$  decreases from 100 % when  $(\kappa + \sigma) d = 0$  to 0 % for infinite thickness. The transmittance has been plotted on a logarithmic scale to test the exponential behaviour of the curves.

For the high absorption cases ( $\kappa/\sigma \geq 20$ ) the behaviour of  $T$  fits the Beer's law

$$T = \exp[-(\kappa + \sigma) d].$$

For the intermediate cases ( $10^{-1} < \kappa/\sigma < 2$ ), the behaviour of  $T$  is still nearly exponential but the slope of the  $\text{Ln}(T)$  curves as a function of the optical thickness varies continuously from  $-1$  to about  $-0.5$  when  $\kappa/\sigma$  decreases from 20 to  $10^{-1}$ . A detailed analysis of the data shows that this remains true even for optical thicknesses as small as 0.05.

For the highly scattering cases ( $10^{-3} < \kappa/\sigma < 10^{-1}$ ) the slope of the  $\text{Ln}(T)$  curves remains very close to 0.5 for very small thicknesses. But as  $(\kappa + \sigma) d$  increases, the curves begin to bend and the behaviour is exponential only for large optical thicknesses with slopes that can be extremely small ( $-0.06$  for  $\kappa/\sigma = 10^{-3}$ ). From these observations it appears that a measurement of the slope of the  $\text{Ln}(T)$  curve as a function of  $d$  is not sufficient to determine separately  $\kappa$  and  $\sigma$  if  $\kappa/\sigma$  is unknown.

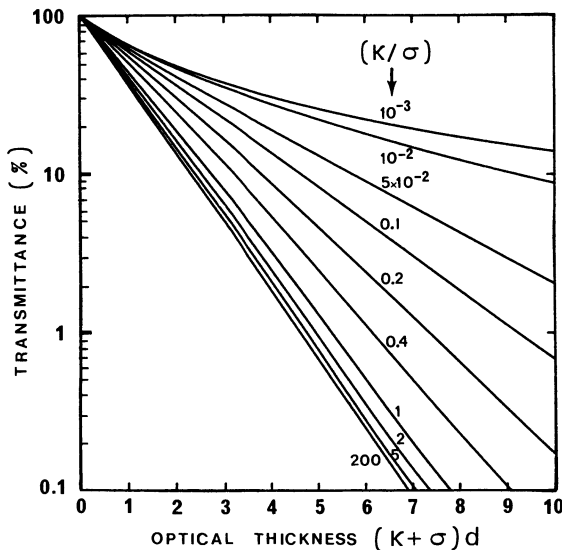


Fig. 4. — MC calculated transmittance as a function of optical thickness for  $\kappa/\sigma$  ranging from  $10^{-3}$  to  $2 \times 10^2$ . Isotropic scattering; Normally incident collimated beam; Index matching.

Table I. — *Some MC calculated values of transmittance (%) for an isotropic scattering medium illuminated by a normally incident collimated beam. Index matching.*

T (%)		Optical thickness ( $\kappa + \sigma$ ) d							
		0.05	0.1	0.2	0.5	1	2.5	5	10
$\kappa/\sigma$	$10^{-3}$	97.54	95.26	90.87	79.74	65.72	42.22	25.75	13.87
	$5 \times 10^{-3}$	97.53	95.19	90.80	79.61	65.45	41.26	23.91	10.98
	$10^{-2}$	97.52	95.23	90.79	79.40	65.07	40.24	22.09	8.57
	$5 \times 10^{-2}$	97.45	94.98	90.30	78.12	62.40	33.85	13.08	2.04
	$10^{-1}$	97.33	94.75	89.84	76.80	59.64	28.55	8.32	0.68
	$2 \times 10^{-1}$	97.11	94.30	88.92	74.65	55.61	22.47	4.62	0.17
	$5 \times 10^{-1}$	96.61	93.47	87.22	70.66	49.10	15.59	2.06	1.03
	1	96.31	92.62	85.76	67.43	44.56	12.24	1.31	0.01
	2.5	95.78	91.69	83.85	64.11	40.56	9.87	0.90	0.01
	5	95.48	91.15	92.99	62.56	38.78	9.06	0.78	0.01
	10	95.31	90.87	82.51	61.61	37.81	8.67	0.71	0
	20	95.26	90.72	82.25	61.13	37.30	8.42	0.69	0
100	95.11	90.54	81.96	60.60	36.95	8.26	0.69	0	

Table II. — *Some calculated values of reflectance (%) for an isotropic scattering medium illuminated by a normally incident collimated beam. Index matching.*

R (%)		Optical thickness ( $\kappa + \sigma$ ) d							
		0.05	0.1	0.2	0.5	1	2.5	5	10
$\kappa/\sigma$	$10^{-3}$	2.45	4.73	9.10	20.18	34.11	57.29	73.14	83.84
	$5 \times 10^{-3}$	2.44	4.76	9.08	20.04	33.74	56.32	70.88	79.04
	$10^{-2}$	2.42	4.70	9.00	19.90	33.34	55.05	68.06	74.12
	$5 \times 10^{-2}$	2.29	4.49	8.56	18.63	30.36	46.71	53.23	54.30
	$10^{-1}$	2.18	4.24	8.00	17.21	27.38	39.55	42.90	43.24
	$2 \times 10^{-1}$	2.00	3.86	7.22	14.94	22.88	30.60	31.93	32.04
	$5 \times 10^{-1}$	1.56	2.97	5.46	10.72	15.32	18.62	18.89	18.94
	1	1.14	2.19	3.87	7.30	9.93	11.44	11.54	11.53
	2.5	0.64	1.20	2.10	3.70	4.83	5.37	5.38	5.37
	5	0.38	0.69	1.18	2.06	2.60	2.86	2.86	2.87
	10	0.20	0.37	0.63	1.09	1.36	1.48	1.48	1.48
	20	0.10	0.19	0.33	0.55	0.69	0.75	0.75	0.76
100	0.02	0.04	0.07	0.11	0.14	0.15	0.15	0.15	

When  $\kappa/\sigma$  tends toward zero the variations of  $T$  can be approximate to the formula :

$$T = \frac{1}{2} \frac{3 - \exp(-(\kappa + \sigma) d)}{1 + (\kappa + \sigma) d}$$

given by Reichman [19] for the isotropic normal conservative case. For example if  $\kappa/\sigma = 10^{-3}$  the relative discrepancy between the MC results and this formula is less than  $10^{-3}$  for optical thicknesses smaller than 1 and is not greater than 3 percent for larger thicknesses.

For very small thicknesses the Reichman formula reduces to  $T = 1 - 0.5 (\kappa + \sigma) d \approx 1 - R$  when  $\kappa d$  is negligible. This limit formula illustrates the fact that, in the isotropic case, a scattered photon has an equal probability to leave the medium forward or downward.

Figure 5 shows the calculated reflectance  $R$  as a function of  $(\kappa + \sigma) d$ .  $R$  increases from 0 % when  $(\kappa + \sigma) d = 0$  to an asymptotic value  $R_\infty$  for infinite thickness. This limit value  $R_\infty$  is reached more rapidly as  $\kappa/\sigma$  increases. The optical thickness has been plotted on a logarithmic scale to show this behaviour : the random path-way followed by the photon can return to the illuminated surface. This phenomenon is more probable if the optical thickness is large and if the absorption is low. The asymptotic value  $R_\infty$  is due to the fact that a photon venturing deeply inside the sample has a poor chance of returning back to the surface.

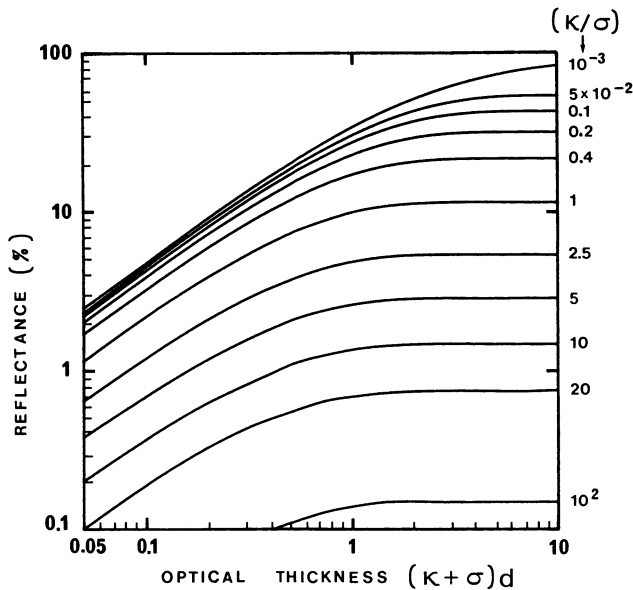


Fig. 5. — MC calculated reflectance as a function of optical thickness for  $\kappa/\sigma$  ranging from  $10^{-3}$  to  $10^2$ . Isotropic scattering ; Normally incident collimated beam ; Index matching.

For  $(\kappa + \sigma) d < 1$  and  $\kappa/\sigma < 10^{-1}$ , the behaviour of  $R$  tends to become independent of  $\kappa/\sigma$ .

Figure 6 shows the results concerning the fraction  $A = 1 - (R + T)$  of the incident light absorbed in the medium. The absorbance  $A$  increases from 0 % for  $(\kappa + \sigma) d = 0$  to  $(1 - R_\infty)$  for infinite thickness.

If  $\kappa/\sigma \geq 20$  then  $A \approx 1 - T \approx 1 - \exp[-(\kappa + \sigma) d]$ .

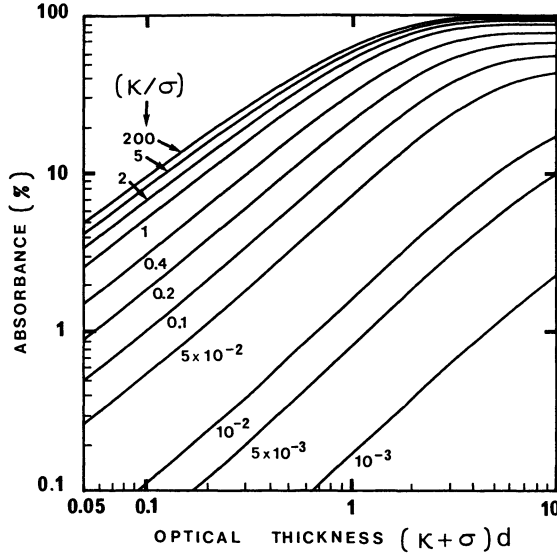


Fig. 6. — MC calculated absorbance as a function of optical thickness for  $\kappa/\sigma$  ranging from  $10^{-3}$  to  $2 \times 10^2$ . Isotropic scattering ; Normally incident collimated beam ; Index matching.

In this very simple case some accurate values of  $R$  and  $T$  can be found in tabulations by Van De Hulst [6] and Giovanelli [22]. In all cases the absolute deviation, between our MC results and these values, is smaller than the absolute statistical error of our MC calculations, that is  $5 \times 10^{-4}$ .

3.2 COMPARISON WITH ANALYTICAL EXPRESSIONS.

3.2.1 *Two or three-flux phenomenological models.* — The well known Kubelka and Munk (KM) 2-flux model [3] can be used when the sample is illuminated by diffuse light and when the homogeneous scattering medium is bounded by parallel planes and extends over a region very large compared to its thickness. These restrictions eliminate two dimensions from the problem. In this model, light in the medium is separated into two diffuse fluxes propagating forwards ( $F_+$ ) and outwards ( $F_-$ ). These two fluxes are coupled by two first order differential equations :

$$\begin{aligned} dF_+/dz &= - (K + S) F_+ + SF_- \\ -dF_-/dz &= - (K + S) F_- + SF_+ \end{aligned} \tag{3}$$

where the direction  $z$  is perpendicular to the slab surfaces,  $z = 0$  at the illuminated surface. The KM absorption ( $K$ ) and back scattering ( $S$ ) coefficients for the diffuse fluxes  $F_+$  and  $F_-$  are different from the coefficients  $\kappa$  and  $\sigma$  used in transport theory. The relations between the KM coefficients and  $\kappa$  and  $\sigma$  have been studied for isotropic scattering by Klier [11] and Meador and Weaver [12].

When there are no surface reflections, equations (3) are solved for the following boundary conditions :

$$\begin{aligned} F_+(z = 0) &= I_d \\ F_-(z = d) &= 0 \end{aligned} \tag{4}$$

where  $I_d$  is the incident diffuse light. The well known solutions for the reflectance  $R_{2F} = F_-(z = 0)/I_d$  and the transmittance  $T_{2F} = F_+(z = d)/I_d$  are :

$$\begin{aligned} R_{2F} &= G \times [1 - \exp(-2 \mu d)] / [1 - G^2 \exp(-2 \mu d)] \\ T_{2F} &= (1 - G^2) \times \exp(-\mu d) / [1 - G^2 \exp(-2 \mu d)] \end{aligned} \tag{5}$$

where

$$\mu = [K(K + 2S)]^{1/2} \quad \text{and} \quad G = (K + S - \mu) / S.$$

The reflectance of a semi-infinite slab is  $R_{2F}^\infty = G$ .

This two-flux model is still often used for measurements of optical characteristics of materials with collimated incident light rather than diffuse light as required by the theory [13, 20]. This is due to the main advantages of this model : equations (5) are very simple and it is possible to calculate  $K$  and  $S$  from  $T$  and  $R$  measurements with simple analytical relations [15]. The most familiar argument for such a use is that the incident collimated beam is rapidly converted into diffuse light. This argument seems *a priori* quite poor because, as can be seen from figures 4 and 5, an important part of the significant events takes place in the first optical depth where, for instance, the absorption of ideally diffuse light is twice the absorption of collimated light.

A comparison of the results obtained from equations (5) with the exact results of MC calculations for normally incident collimated light is shown in figure 7. The ratios of the values calculated by the 2-flux and MC2 theories are mapped as a function of  $(\kappa + \sigma) d$  and  $\kappa/\sigma$ .

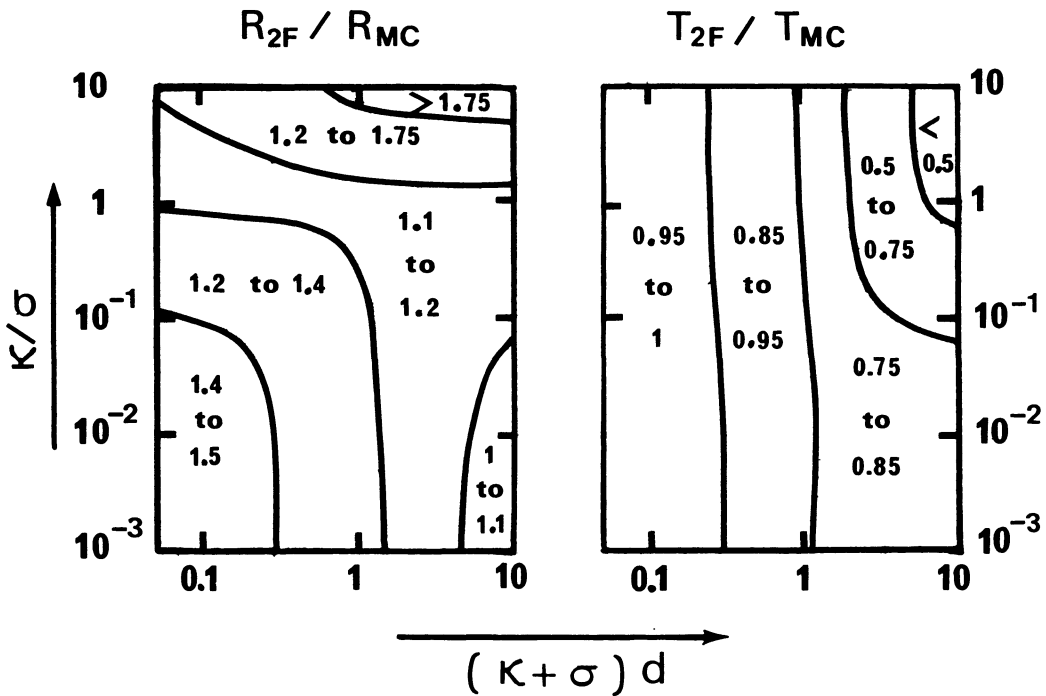


Fig. 7. — Ratio of the reflectances (or transmittances) calculated by the two flux theory and the Monte Carlo method for collimated normally incident beam, mapped as a function of  $(\kappa + \sigma) \times d$  and  $\kappa/\sigma$ . Isotropic scattering and index matching.

$\kappa/\sigma$ . These parameters have been derived from  $K$ ,  $S$  and  $d$  by using the analytical equations given by Meador and Weaver [12]:

$$\kappa = \eta K$$

$$\sigma = \chi S$$

$$224 \eta = 77 + 55 \varepsilon + 35 [1 + (2 \varepsilon/35) + (121 \varepsilon^2/49)]^{1/2} \quad (6)$$

$$\chi = 2 \eta (1 - \varepsilon) (16 \eta - 3) / [15 \eta^2 - \varepsilon(16 \eta - 3)].$$

Which are in excellent agreement with the results of Klier [11] if  $\kappa/\sigma < 1$ .

It is seen that if  $\kappa/\sigma < 1$ , the ratio  $R_{2F}/R_{MC}$  is very different from 1 for the small optical thicknesses and becomes closer to 1 as  $(\kappa + \sigma) d$  increases. If  $\kappa/\sigma < 0.1$  and  $(\kappa + \sigma) d > 5$  a better fit occurs (proportional deviation  $< 10\%$ ). The best agreement is obtained with the larger optical thicknesses and the smaller absorption coefficients. If the absorption is significant ( $\kappa/\sigma > 1$ ) the deviation is always larger than  $10\%$  and increases as  $(\kappa + \sigma) d$  increases.

On the contrary, for transmittances the agreement is good only for small optical thicknesses, that is when the absorbance of the sample is negligible, and the proportional deviation increases rapidly as  $(\kappa + \sigma) d$  increases.

This comparison shows that the use of the 2-flux model should be avoid when the incident light is collimated.

In the case of collimated illumination by an incident parallel beam much broader than  $d$  to remain in a one dimensional problem, and when there are no reflections at the boundaries, it is in fact necessary to insert in equations (3) a third flux  $I_C$  representing the unscattered collimated beam within the medium [16-18]: the two diffuse fluxes  $F_+$  and  $F_-$  are augmented by the light scattered from this primary collimated beam. In case of isotropic scattering, equations (3) become:

$$\begin{aligned} dI_C/dz &= -(\kappa + \sigma) I_C \\ dF_+/dz &= \frac{\sigma}{2} I_C - (K + S) F_+ + S F_- \\ -dF_-/dz &= \frac{\sigma}{2} I_C - (K + S) F_- + S F_+ \end{aligned} \quad (7)$$

The boundary conditions are:

$$\begin{aligned} I_C(z=0) &= I_0 \\ F_+(z=0) &= 0 \\ F_-(z=d) &= 0 \end{aligned} \quad (8)$$

where  $I_0$  is the intensity of the collimated incident beam.

The solutions for the reflectance  $R_{3F} = F_-(z=0)/I_0$  and the transmittance  $T_{3F} = [I_C(z=d) + F_+(z=d)]/I_0$  are:

$$\begin{aligned} R_{3F} &= C R_{2F} + D T_{2F} \exp(-\gamma d) - D \\ T_{3F} &= C T_{2F} + D R_{2F} \exp(-\gamma d) + (1 - C) \exp(-\gamma d) \end{aligned} \quad (9)$$

where  $\gamma = \kappa + \sigma$ ,

$$C = (\sigma/2)(\kappa + 2S + \gamma)/(\gamma^2 - \mu^2)$$

and

$$D = (\sigma/2)(\kappa + 2S - \gamma)/(\gamma^2 - \mu^2).$$

The reflectance of a semi-infinite slab is  $R_{3F}^\infty = CR_{2F}^\infty - D$ .

The light distribution within the medium is given by :

$$I(z) = [(1 - C - D) \exp(-\gamma z) + Ch(d - z) + Dh(z) \exp(-\gamma d)] I_0 \quad (10)$$

where :

$$h(z) = [(1 + G) + G(1 - G) \exp(-2\mu z)] / [1 - G^2 \exp(-2\mu z)] .$$

A comparison of the results obtained from equations (9) with the exact results of MC calculations is shown in figure 8. Once more equations (6) have been used to relate  $K$  and  $S$  to  $\kappa$  and  $\sigma$  in spite of the fact that they were settled for ideally diffuse illumination.

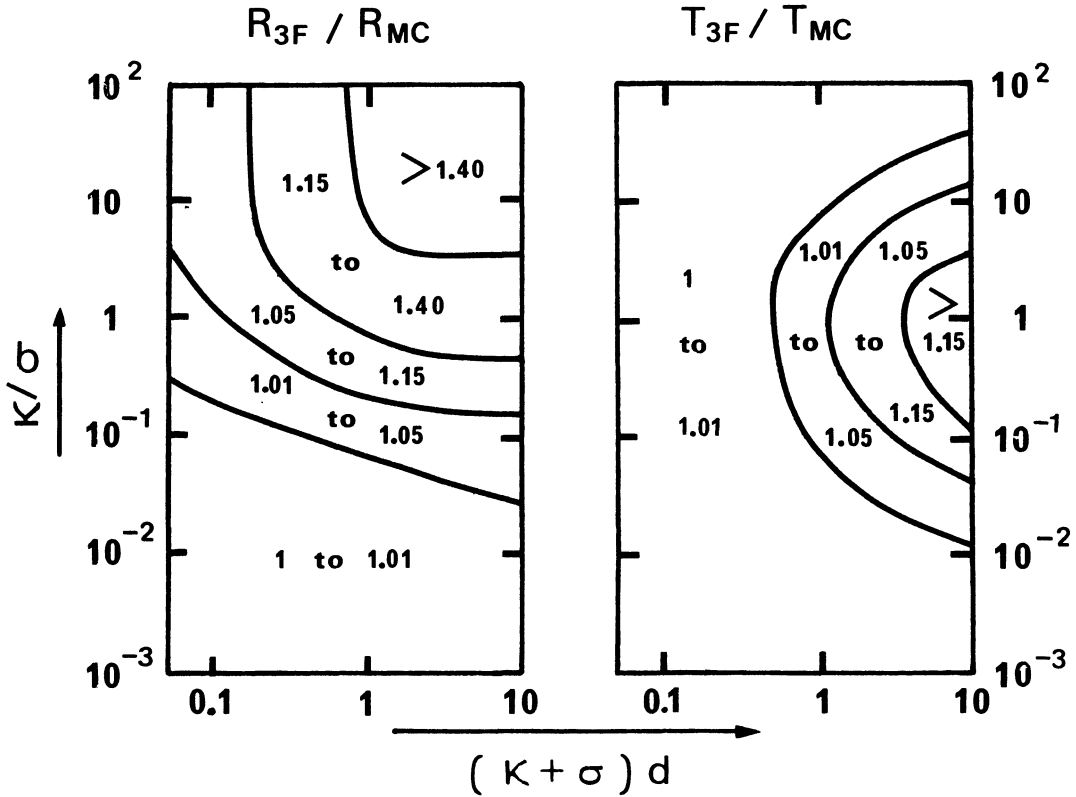


Fig. 8. — Ratio of the reflectances (or transmittances) calculated by the three theory and the Monte Carlo method mapped as a function of  $(\kappa + \sigma) \times d$  and  $\kappa/\sigma$ . Isotropic scattering ; Normally incident collimated beam ; Index matching.

For transmittances, both methods give values very close to the Beer's law in the high absorption cases ( $\kappa/\sigma \geq 20$ ). In the high scattering situations ( $\kappa/\sigma < 10^{-2}$ ) the fit is also excellent for any optical thickness. In the intermediate case ( $10^{-2} < \kappa/\sigma < 20$ ), a deviation occurs for large optical thicknesses, but it remains smaller than 5% if  $(\kappa + \sigma)d < 1$ .

For reflectances, the agreement is good only in the high scattering cases ( $\kappa/\sigma < 10^{-1}$ ) and becomes very poor as  $\kappa/\sigma$  increases.

3.2.2 *Analytical expressions derived from diffusion theory.* — From the equation of radiation transfer :

$$\begin{aligned} \mu \frac{dI(\mu)}{d\tau} = & -I(\mu) + \frac{\omega_0}{4\pi} \exp(-\tau/\mu_0) \int_{-1}^1 \int_0^{2\pi} p(\mu, \varphi, \mu', \varphi') \delta(\mu - \mu_0) d\mu' d\varphi' \\ & + \frac{\omega_0}{4\pi} \int_{-1}^1 \int_0^{2\pi} I(\mu') p(\mu, \varphi, \mu', \varphi') d\mu' d\varphi' \end{aligned}$$

and using the Schuster-Schartzchild approximation, Reichman [19] has derived from the equation of radiation transfer explicite expressions for the reflectances and transmittances of homogeneous materials illuminated by a collimated beam. When the phase function is constant (isotropic scattering) and for normal incidence, the equations reduce to :

$$\begin{aligned} R_{\mathfrak{R}} = & (\omega_0/2)[3\Gamma + (1 - \Gamma^2) \exp[-(1 + \alpha)\gamma d] - 1 \\ & - \Gamma(3 - \Gamma) \exp[-2\alpha\gamma d]] / [(1 - \alpha^2)(1 - \Gamma^2 \exp[-2\alpha\gamma d])] \\ T_{\mathfrak{R}} = & (\omega_0/2)[3(1 - \Gamma^2) \exp[-\alpha\gamma d] - (3 - \Gamma) \exp[-\gamma d] \\ & + \Gamma(3\Gamma - 1) \exp[-(1 + 2\alpha)\gamma d]] / [(1 - \alpha^2)(1 - \Gamma^2 \exp[-2\alpha\gamma d])] \\ & + \exp[-\gamma d] \end{aligned} \quad (11)$$

where

$$\omega_0 = \sigma / (\kappa + \sigma), \quad \alpha = 2(1 - \omega_0)^{1/2} \quad \text{and} \quad \Gamma = (2 - \alpha) / (2 + \alpha).$$

The reflectance of a semi-infinite slab is :

$$R_{\mathfrak{R}}^{\infty} = \omega_0(3\Gamma - 1) / 2(1 - \alpha^2) \quad (12)$$

it can be noticed that the optical thickness  $\gamma d$  appears only in the exponentials and that the other coefficients depend only on the albedo  $\omega_0$  that is on the ratio  $\kappa/\sigma$ .

The advantage of this model over the 3-flux model is that it does not require the use of the  $K$  and  $S$  Kubelka and Munk coefficients.

Figure 9 shows a comparison of the results obtained from (11) with those of MC calculations :

For transmittances the fit is excellent for all  $\kappa/\sigma$  values if  $(\kappa + \sigma)d < 2$  (proportional deviation  $< 1\%$ ) but the deviation increases very quickly if  $(\kappa + \sigma)d > 2$  especially for intermediate values of  $\kappa/\sigma$ .

For the reflectances, the agreement is much better than in figure 8 for the high absorption cases and for the large optical thicknesses. If  $\kappa/\sigma < 0.3$  the deviation remains lower than 5% whatever is the optical thickness and if  $\kappa/\sigma > 0.3$  the deviation is lower than 15%.

3.2.3 *Comparison of the analytical expressions.* — It is very interesting to notice that the equations (11) derived from the equation of radiative transfer are equivalent to the 3-flux expressions (9) if the following identifications are made :  $K = 2\kappa$ ,  $S = \sigma$ . Then  $\mu = \alpha\gamma$ ,  $G = \Gamma$ ,  $C = 3D = 3\omega_0/2(1 - \alpha^2)$  and one can write :

$$\begin{aligned} R_{\mathfrak{R}} = & R_{3F}(\eta = 0.5, \chi = 1) \\ T_{\mathfrak{R}} = & T_{3F}(\eta = 0.5, \chi = 1). \end{aligned}$$

The comparisons shown in figure 8 and figure 9 demonstrate clearly that the results obtained with a multi-flux model depend strongly on the choice of the Kubelka-Munk coefficients  $K$  and  $S$ . This problem has been widely discussed in the case of diffuse light illumination [4, 11, 12, 20, 21] and also for collimated illumination [4]. Relations between the KM coefficients and  $\kappa$  and  $\sigma$  have been obtained by identification between KM equations and

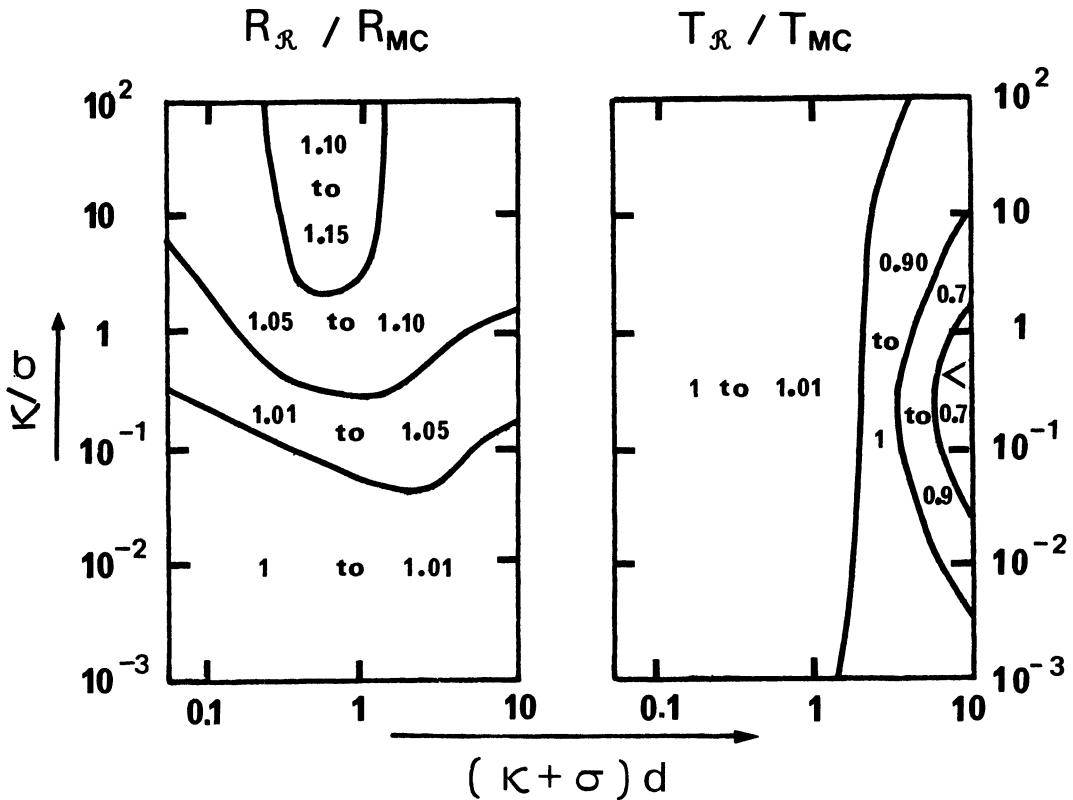


Fig. 9. — Ratio of the reflectances (or transmittances) calculated by equations (11) and the Monte Carlo method mapped as a function of  $(\kappa + \sigma) \times d$  and  $\kappa/\sigma$ . Isotropic scattering; Normally incident collimated beam; Index matching.

solutions of the radiative transfer equation. The disagreement between the KM coefficients so obtained and those previously deduced from physical arguments was in some cases resolved [5, 21] by using different coefficients for different flux directions. In reality, the main problem comes from the fact that  $K$  and  $S$  are not independent of the position  $z$  within the sample [21] and that there is no simple way to correct the KM equations for the effects of this dependence.

In practice and from the results shown in figure 8 and figure 9 we observe that :

- 1) if  $\kappa/\sigma < 10^{-2}$ , the values of  $T$  and  $R$  obtained with the 3-flux model and the equations (6) given by Meador and Weaver [12] are excellent for any optical thickness ;
- 2) the equations (11) derived by Reichman ( $\eta = 0.5, \chi = 1$ ) give very good results for  $R$  in almost all cases ;
- 3) if  $(\kappa + \sigma)d < 1$  both methods compare well with MC results for  $T$ .

One interesting point is that in MC calculations, no assumption has been made about the width of the incident collimated beam. Therefore, the 3-flux model can be used to calculate the total reflectance or transmittance even if the incident beam is very thin. Of course, this would not be true for the calculation of the light distribution within the medium.

Since 3-flux  $R$  and  $T$  calculations can be done in a few seconds on a personal computer they are recommended for use whenever their accuracy is acceptable. If  $\kappa$  and  $\sigma$  are known, figure 8 and figure 9 can be used to determine their range of reliability and have a first idea of the correction that should be made.

If the accuracy is not sufficient, MC calculations give in any case results that are as reliable as the best experimental data. Even though the MC method requires much more computer time it is rapid enough to be used as a current tool in laboratories : the average computation time for one group of photons varies, for a semi-infinite slab of isotropic scattering material, from  $2 \times 10^{-3}$  s to 0.2 s when  $\kappa/\sigma$  varies from  $10^2$  to  $10^{-2}$ . This time is strongly reduced when the optical thickness is smaller.

However, it should be noted that in the very simple case considered here (plane-parallel slab, normally incident collimated beam, isotropic scattering), other numerical methods, as the doubling method [6], could be faster and as accurate as MC if all what is required is  $R$  and  $T$ . But these methods would not be suitable for other geometries.

**3.3 DIRECT DETERMINATION OF  $\kappa$  AND  $\sigma$  FROM  $R$  AND  $T$  MEASUREMENTS.** — The 2-flux model based on the boundary condition of diffuse incident radiation is widely used to extract the optical properties of a medium from  $R$  and  $T$  measurements because explicit expressions for  $K$  and  $S$  as functions of  $R$  and  $T$  are available. But beside the fact that diffuse illumination is difficult to perform (especially for  $R$  measurements) we have seen that an additional shortcoming of these models is that the parameters  $K$  and  $S$  require delicate interpretation to relate them to  $\kappa$  and  $\sigma$ . Since spectroscopic measurements are normally made with collimated incident radiation, it is more convenient to use models developed for such an illumination.

When the sample is illuminated by a normally incident collimated beam, equations (11) are very simple but we have not been able to invert them in order to find analytical expressions giving  $\kappa$  and  $\sigma$  as functions of  $R$  and  $T$ . Nevertheless commercially available programs may be used to perform a numerical inversion of these expressions in a few seconds. To determine approximate values of  $\kappa$  and  $\sigma$  from the knowledge of  $R$ ,  $T$  and  $d$  we have used the program Eureka of Borland with equations (11). The precision of the results, as tested with accurate MC calculations depends strongly on  $\kappa$ ,  $\sigma$  and  $d$ . This is due to the deviations observed in figure 9 and also to some other undeterminations that are discussed below.

In order to surmount these difficulties we have constructed a diagram (Fig. 10) with accurate MC values of  $R$  and  $T$ . The axis of abscissa is a logarithmic scale of the optical thickness ranging from 0.05 to 10 and the axis of ordinate is a logarithmic scale of  $\kappa/\sigma$  ranging from  $10^{-2}$  and  $10^2$ . A first family of curves represents constant values of  $R$  and a second family of curves represents constant values of  $T$ . The coordinates of the intersection of two  $R$  and  $T$  curves give the corresponding value of  $\kappa/\sigma$  and  $(\kappa + \sigma)d$ . It is then easy to calculate  $\kappa$  and  $\sigma$  if the sample thickness  $d$  can be measured.

For the sake of clarity a limited number of  $R$  and  $T$  curves are shown in figure 10. In the area where the meshes are tight, approximate values of  $(\kappa + \sigma)d$  and  $\kappa/\sigma$  can be obtained very rapidly and only a few more MC calculations are necessary to reach an accuracy compatible with the precision of the measurements (For numerical extrapolations one can see Tab. I and Tab. II).

If the absorbed energy is smaller than 5 % of the incident light, that is in the area below the dotted line in figure 10 corresponding to  $A = 1 - (R + T) = 5\%$ , the meshes are stretched out along the ordinate axis leading to a greater undetermination of  $\kappa/\sigma$ . This is due to the fact that, as can be seen in figure 4 and figure 5,  $R$  and  $T$  tend to become independent of  $\kappa/\sigma$  in the high scattering case ( $\kappa/\sigma < 10^{-1}$ ) and for the small optical thicknesses ( $(\kappa + \sigma)d < 1$ ).

Using equations (11), which give excellent results in this area, we obtain :

$$\begin{aligned} R_{\mathcal{R}} &\rightarrow R_{\mathcal{R}}^{\text{lim}} = (1/2)[2 \gamma d - 1 + \exp(-\gamma d)]/(\gamma d + 1) \\ T_{\mathcal{R}} &\rightarrow T_{\mathcal{R}}^{\text{lim}} = (1/2)[3 - \exp(-\gamma d)]/(\gamma d + 1) \end{aligned} \quad (13)$$

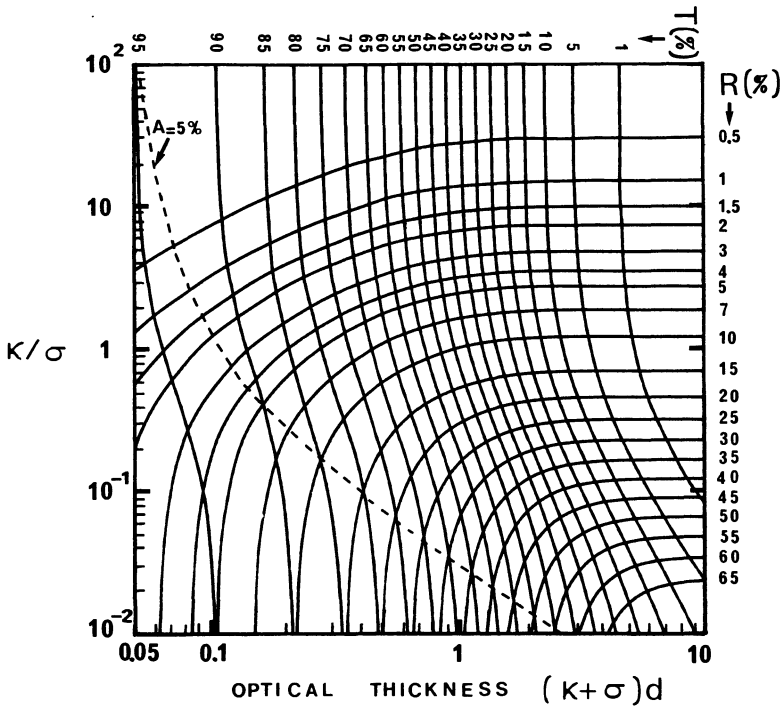


Fig. 10. — Monte Carlo calculations diagram for direct graphical determination of  $\kappa/\sigma$  and  $(\kappa + \sigma) \times d$  for  $R$  and  $T$  measurements. A first set of curves corresponds to constant  $R$  values and a second set corresponds to constant  $T$  values. The coordinates of the intersection of two  $R$  and  $T$  curves give the corresponding values of  $\kappa/\sigma$  and  $(\kappa + \sigma) \times d$ . Normally incident collimated beam ; Isotropic scattering ; Index matching. The dotted line corresponds to  $A = 1 - R - T = 5\%$ .

where  $R_r^{\text{lim}}$  and  $T_r^{\text{lim}}$  depend only on the optical thickness  $\gamma d$ .

A comparison of equation (13) with accurate MC calculations is given in table III for  $\kappa/\sigma = 10^{-2}$  and  $\kappa/\sigma = 10^{-3}$ . It is seen that the absolute deviation of  $R$  and  $T$  from their limit values is smaller than 0.01 if  $(\kappa + \sigma) d < 1$ . Measurements made on these conditions can be used for an accurate determination of the optical thickness but the usual experimental precision is not sufficient to determine precisely  $\kappa/\sigma$ .

This problem is also encountered in the area where  $R < 0.5\%$  that is in the high absorption cases ( $\kappa/\sigma > 20$ ) for which the behaviour of  $T$  fits the Beer's law  $T \approx \exp(-\gamma d)$  whatever is the optical thickness. The reflectance in this area is not much greater than the accuracy of the best commercially available reflectance spectrometers and the determination of  $\kappa/\sigma$  is difficult.

If the transmittance is smaller than 10%, that is on the right side of the curve  $T = 10\%$  in figure 10, the reflectance is very close to the asymptotic value  $R_\infty$  for infinite thickness. In this area  $\kappa/\sigma$  is determined by the measurement of  $R$  even if the thickness  $d$  is unknown. The inversion of equation (12) gives a very simple relation between  $R_\infty$  and  $\kappa/\sigma$  :

$$\kappa/\sigma = (1 - R_\infty)^2 / 3 R_\infty (R_\infty + 2) . \tag{14}$$

Table III. — *High scattering cases and small optical thicknesses : comparison of reflectances and transmittances calculated by the Monte Carlo method with the limit values obtained with equation (13).*

$\kappa/\sigma$	Optical Thickness ( $\kappa + \sigma$ ) $d$	Reflectance		Transmittance	
		Exact $R_{MC}$	Limit $R_{\kappa}^{\text{lim}}$	Exact $T_{MC}$	Limit $T_{\kappa}^{\text{lim}}$
$10^{-2}$	0.05	0.0242	0.0244	0.9752	0.9756
	0.1	0.0470	0.0477	0.9523	0.9519
	0.5	0.1990	0.2022	0.7940	0.7978
	1	0.3334	0.3420	0.6507	0.6580
	5	0.6806	0.7506	0.2209	0.2494
$10^{-3}$	0.05	0.0245	0.0244	0.9754	0.9756
	0.1	0.0473	0.0477	0.9526	0.9519
	0.5	0.2018	0.2022	0.7974	0.7978
	1	0.3411	0.3420	0.6572	0.6580
	5	0.7314	0.7506	0.2575	0.2494

This relation is tested with accurate MC calculations ( $10^6$  photons) in table IV. The first column gives the exact values of  $\kappa/\sigma$  and the second column gives the corresponding values of  $R_{MC}^{\infty}$  calculated with the MC method for infinite thickness.  $R_{MC}^{\infty}$  is used in equation (14) to calculate  $\kappa/\sigma$ . The error column gives the relative amount by which this calculated value of

Table IV. — *Evaluation of the  $\kappa/\sigma$  values calculated with equation (14). The accurate Monte Carlo values of  $R$  for infinite thickness  $R_{MC}^{\infty}$  are used for this evaluation.*

Exact $\kappa/\sigma$	$R_{MC}^{\infty}$	Calculated $\kappa/\sigma$ . Eq. (14)	Relative Error (%)
$1 \times 10^{-3}$	0.9130	$0.95 \times 10^{-3}$	5.0
$5 \times 10^{-3}$	0.8169	$4.86 \times 10^{-3}$	2.9
$1 \times 10^{-2}$	0.7527	$0.98 \times 10^{-2}$	2.0
$5 \times 10^{-2}$	0.5430	$5.04 \times 10^{-2}$	0.8
$1 \times 10^{-1}$	0.4324	$1.02 \times 10^{-1}$	2.0
$5 \times 10^{-1}$	0.1894	$5.28 \times 10^{-1}$	5.6
1	0.1153	1.07	7.0
1.5	0.0834	1.61	7.3
2	0.0655	2.15	7.5
2.5	0.0537	2.71	8.4
5	0.0287	5.40	8.0
10	0.0148	10.85	8.5
20	0.0076	21.5	7.5
100	0.0015	111	11.0

$\kappa/\sigma$  differs from the exact value given in the first column. The relative difference between the two sets of  $\kappa/\sigma$  values is always smaller than 11 % and for  $\kappa/\sigma < 0.1$  it becomes smaller than 5 %. When  $\kappa/\sigma$  is determined, one can easily calculate the corresponding  $T$  curve as a function of  $(\kappa + \sigma)d$  and extract  $\kappa$  and  $\sigma$  values from the measurements of  $T$  and  $d$ . If  $T$  is too small in comparison with the experimental accuracy, another measurement should be made with a smaller thickness  $d$ .

**4. Effects of reflecting boundaries.**

If the refractive index  $n$  of the medium is different from the environment index  $n'$ , surface reflections, both internal and external must be considered. These reflections depend on the ratio  $n/n'$  of the refractive indices and on the state of the surfaces. Throughout part 4, we use the symbol  $\mathcal{R}$  for the reflectance and  $\mathcal{C}$  for the transmittance.

We present here MC calculations for  $n/n' = 1.4$ . The surfaces of the slab of material are assumed to be sufficiently smooth so that specular reflection occurs. At each reflection the weight of the photons group is multiplied by the reflection coefficient corresponding to its angle of incidence and calculated by Fresnel's equations for unpolarized light (See Fig. 2 and Fig. 3).

Results are shown in figure 11 and figure 12.

The part  $r \times I_0$  of the incident collimated beam externally reflected at the front (illuminated) surface is not included in  $\mathcal{R}$

$$r = [(n - n') / (n + n')]^2 = 0.028 \text{ if } n / n' = 1.4 .$$

If the optical thickness tends to zero,  $\mathcal{R}$  tends to an asymptotic value  $\mathcal{R}_0$  due to successive internal reflections of the collimated beam and independent of  $\kappa/\sigma$

$$\mathcal{R}_0 = r(1 - r)(1 + r^2 + r^4 + \dots) = 2.72 \% \text{ if } n / n' = 1.4 .$$

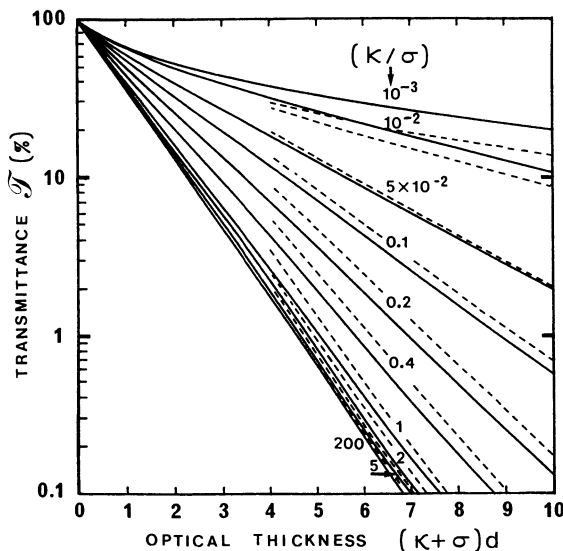


Fig. 11. — MC calculated transmittance as a function of optical thickness. Index ration  $n/n' = 1.4$  ; Specularly reflecting surfaces ; Normally incident collimated beam ; Isotropic scattering. The dotted lines correspond to the results obtained in the matched-boundary case.

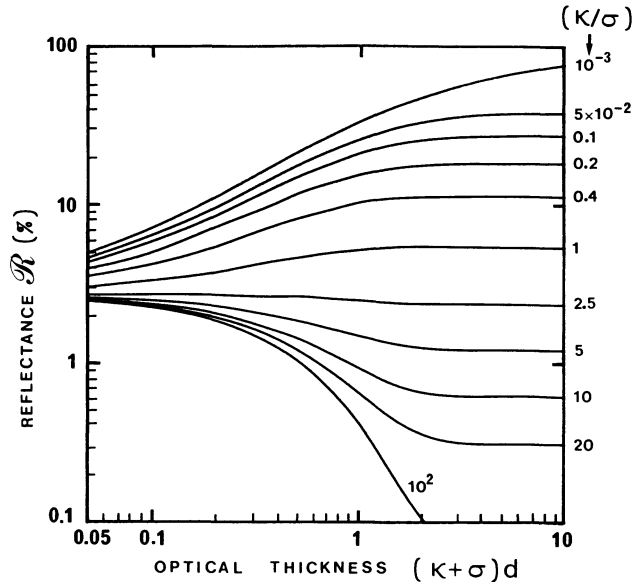


Fig. 12. — MC calculated reflectance as a function of optical thickness. Index ratio  $n/n' = 1.4$ ; Specularly reflecting surfaces; Normally incident collimated beam; Isotropic scattering.

When  $(\kappa + \sigma)d$  increases,  $\mathcal{R}$  tends to an asymptotic value  $\mathcal{R}_\infty$  which is always smaller than the asymptotic value  $R_\infty$  obtained in case of index matching as predicted by Giovanelli [22].

$\mathcal{C}$  decreases from  $(1 - \mathcal{R}_0) = 97.28\%$  when  $(\kappa + \sigma)d = 0$  to  $0\%$  for infinite thickness.

If  $(\kappa + \sigma)d \geq 4$ ,  $\mathcal{C}$  is proportional to the transmittance  $T$  obtained in case of index matching: the slope of the  $\text{Ln}(\mathcal{C})$  curves as a function of the optical thickness is equal to the slope of the  $\text{Ln}(T)$  curves shown in dotted lines in figure 11. For the high scattering cases ( $\kappa/\sigma \leq 5 \times 10^{-2}$ ), the transmittance  $\mathcal{C}$  for  $n/n' = 1.4$  is larger than the transmittance  $T$  in case of index matching ( $n/n' = 1$ ). But if  $\kappa/\sigma \geq 5 \times 10^{-2}$ ,  $\mathcal{C}$  is smaller than  $T$ .

A diagram (Fig. 13) has been constructed with MC calculated  $\mathcal{R}$  and  $\mathcal{C}$  values and can be used for graphical determination of  $\kappa$  and  $\sigma$  from  $\mathcal{R}$ ,  $\mathcal{C}$  and  $d$  measurements as indicated in the previous section.

We have not attempted to compare these accurate MC results with 4-flux calculations for the following reasons:

1) In case of reflections at the boundaries, the KM coefficients  $K$  and  $S$  depend on  $\kappa/\sigma$ ,  $z$  and also on  $n/n'$  and there is no simple way to take this dependence into account.

2) It is not possible to obtain accurate information about the coefficients that describe the reflections of the diffuse fluxes on the internal surfaces. Since the propagation through an attenuating sample tends to partly collimate a diffuse beam, even in the isotropic scattering case [21], the use of the internal reflection coefficients tabulated by Orchard [23] for uniformly diffuse incidence would only give approximate results. Therefore the diffuse internal reflection coefficients should be considered as parameters to be determined experimentally.

3) In consequence a large number of empirical coefficients appear in general 4-flux equations and make the arithmetic rather laborious. Furthermore, the minimum number of measurements necessary for a complete knowledge of the optical properties of the material is at least equal to the total number of unknowns.

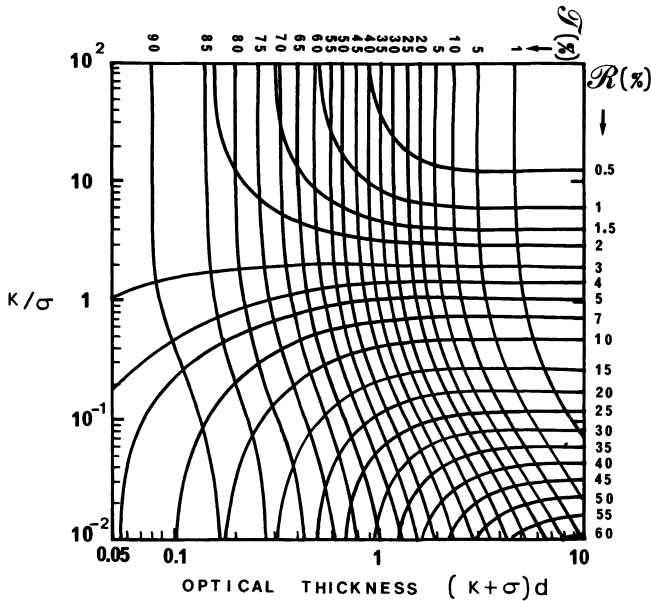


Fig. 13. — MC calculated diagram for direct graphical determination of  $\kappa/\sigma$  and  $(\kappa + \sigma) \times d$  for  $R$  and  $T$  measurements. Index ratio  $n/n' = 1.4$ ; Specularly reflecting surfaces; Normally incident collimated beam; Isotropic scattering.

The main advantage of the MC method over most of the other theories is that reflection is described locally and, in case of specular reflection, the only additional parameter is the indexes ratio  $n/n'$ .

Since  $n$  can be measured by using total reflection in a high index medium, it is easier to spend a few hours in computing a diagram for direct determination of  $\kappa$  and  $\sigma$  from a single  $R$ ,  $C$  and  $d$  measurement rather than to make a large number of measurements leading to the knowledge of empirical parameters.

When the boundaries are not perfectly smooth, reflected or refracted rays are partially diffused depending of the surfaces roughness. There is an infinite range of possibilities when all types of surfaces are considered. This kind of realistic conditions can be easily included in the algorithms of the MC models if the characteristics of the internal reflection are known.

**5. Concluding remarks.**

One of the aims of this paper was to demonstrate that accurate Monte Carlo simulations of light propagation in turbid media can now be performed on commercially available personal computers. The main economical advantage is that the price of these computers is lower than the cost of the computation time on a big computer. Only a few days of effective computation have been necessary to obtain the data used in this paper.

Another interesting point is that accurate purely numerical results if presented by means of sets of curves as a function of physical reduced parameters, can be used to give a comprehensive understanding of the subject. Nevertheless approximate analytical expressions are still very useful because they are computationally fast and also because they provide a way of testing the foundations of numerical models.

No attempt has been made to compare the calculation methods described in this paper with

every accurate numerical solution of the equation of radiative transfer [4, 5]. The Monte Carlo method is chosen here because of its conceptual simplicity and the ease with which realistic conditions can be incorporated in the model.

### References

- [1] GROENHUIS R. A. J., FERWERDA H. A. and TEN BOSCH J. J., Scattering and Absorption of Turbid Materials Determined from Reflection Measurements 1 : Theory, *Appl. Opt.* **22** (1983) 2456.
- [2] LANGERHOLC J., Beam Broadening in Dense Scattering Media, *Appl. Opt.* **21** (1982) 1593.
- [3] KUBELKA P. and MUNK F., Ein Beitrag zur Optik der Farbanstriche, *Z. Tech. Phys.* **12** (1931) 593.
- [4] MUDGETT P. S. and RICHARDS L. W., Multiple scattering Calculations for Technology, *Appl. Opt.* **10** (1971) 1485.
- [5] CHANDRASEKHAR S., Radiative Transfer (Oxford U.P., New York) 1960.
- [6] VAN DE HULST H. C., Multiple Light Scattering, Tables, Formulas and Applications, Vol. 1 (Academic Press, New York) 1980.
- [7] ISHIMARU A., Wave Propagation and Scattering in Random Media, Vol. 1 (Academic, New York) 1978.
- [8] MEIER A. R., LEE J. S. and ANDERSON D. E. Jr., Atmospheric Scattering of Middle UV Radiation from an Internal Source, *Appl. Opt.* **17** (1978) 3216.
- [9] WILSON B. C. and ADAM G., A Monte Carlo model for the Absorption and Flux Distribution in Tissue, *Med. Phys.* **10** (1983) 824.
- [10] HENYEU L. G. and GREENSTEIN J. L., Diffuse Radiation in the Galaxy, *Astrophys. J.* **93** (1941) 70.
- [11] KLIER K., Absorption and Scattering in Plane Parallel Turbid Media, *J. Opt. Soc. Am.* **62** (1972) 882.
- [12] MEADOR W. E. and WEAVER W. R., Diffusion Approximation for Large Absorption in Radiative Transfer, *Appl. Opt.* **18** (1979) 1204.
- [13] WAN S., ANDERSON R. R. and PARRISH J. A., Analytical Modeling for the Optical Properties of the Skin with *in vitro* and *in vivo* Applications, *Photochem. Photobiol.* **34** (1981) 493.
- [14] PRINCE M. R., DEUTSCH T. F., MATHEWS-ROTH M. M., MARGOLIS R., PARRISH J. A. and OSEROFF A. R., Preferential Light Absorption in Atheromas *in vitro*, *J. Clin. Invest.* **78** (1986) 295.
- [15] KUBELKA P., New Contributions of the Optics of Intensely Light Scattering Materials, *J. Opt. Soc. Am.* **38** (1948) 448.
- [16] SILBERSTEIN L., The Transparency of Turbid Media, *Philos. Mag.* **4** (1927) 129.
- [17] RYDE J. W., The Scattering of Light by Turbid Media, *Proc. Roy. Soc. A* **90** (1931) 219 ; *J. Soc. Glass Tech.* **16** (1932) 408.
- [18] DUNTLEY S. Q., The Optical Properties of Diffusing Materials, *J. Opt. Soc. Am.* **32** (1942) 61.
- [19] REICHMAN J., Determination of Absorption and Scattering Coefficients for Nonhomogeneous Media 1 : Theory, *Appl. Opt.* **12** (1973) 1811.
- [20] GATE L. F., Comparison of the Photon Diffusion Model and Kubelka-Munk Equation with the Exact Solution of Radiative Transfer Equation, *Appl. Opt.* **13** (1974) 237.
- [21] LATIMER P. and NOH S. J., Light Propagation in Moderately Dense Particle Systems : a Reexamination of the Kubelka-Munk Theory, *Appl. Opt.* **26** (1987) 514.
- [22] GIOVANELLI R. G., Reflection by Semi-infinite Diffusers, *Opt. Acta Paris* **2** (1955) 153.
- [23] ORCHARD S. E., Reflection and Transmission of Light by Diffusing Suspensions, *J. Opt. Soc. Am.* **59** (1969) 1583.
- [24] MC1 and MC2 programs are available for distribution by the authors.